2010

Effect of internal solitary waves on underwater acoustic propagation

Chu, Peter C.

Chu, P.C., and C.-P. Hsieh, 2010: Effect of internal solitary waves on underwater acoustic propagation. Marine Technology Society Journal, 44 (5), 10-16 (paper download).

PAPER

Effect of Internal Solitary Waves on Underwater Acoustic Propagation

AUTHORS

Peter C. Chu
Chung-Ping Hsieh
Naval Ocean Analysis
and Prediction Laboratory,
Naval Postgraduate School

ABSTRACT

Internal solitary waves (ISWs) were observed on 07:52–09:36 GMT July 30, 2005, in the Philippine Sea near Taiwan from high-resolution temperature sampling. The effect of ISWs on acoustic propagation was identified using the Navy's Comprehensive Acoustic Simulation System through comparison between range-independent and range-dependent sound speed profiles. The ISWs enhance the sound propagation slightly (0–3 dB) in near-range, weaken or enhance the sound propagation (–20 to 20 dB) evidently in midrange, and always weaken the sound propagation (up to –20 dB) in far range. The ISW's effect on the acoustic propagation varies with sound frequency and sound source depth. This work provides a methodology to anticipate possible errors in transmission loss estimation in an operational framework, if no further additional data are available.

Key Words: Acoustic detection, CASS/GRAB, Coastal monitoring buoy, Internal solitary wave, Ray path

Introduction

Nonlinear propagating internal solitary waves (ISWs) are a ubiquitous feature of the coastal ocean. They have been observed as sharp depressions of a near surface pycnocline that are often seen at the surface as alternating bands of slicks and rough patches (i.e., Apel et al., 1985; Chu and Hsieh, 2007b). The effect of ISWs on sound propagation has been investigated extensively in the continental shelves such as the Yellow Sea (Zhou and Zhang 1991) and north of Lisbon (Rodriguez et al. 2000). Zhou and Zhang (1991) claimed that ISWs contribute to an important loss mechanism for shallow water sound propagation. However, Rodriguez et al. (2000) argued that ISWs cause successive signal attenuation and signal amplification (called acoustic focusing). It is noted that the signal attenuation or amplification as observed and modeled by these studies depend on frequency and propagation angle of the nonlinear internal waves.

Usually, the effect of ISWs on sound propagation is masked by boundary interactions. For a deep sea such as the Philippine Sea, the surface and the bottom acoustic interactions are weak. Thus, the effect of ISWs on

FIGURE 1

Topography of the western Philippine Sea and surrounding areas with the symbol "+" indicating the location where the ISWs were observed. Note that the ISWs were observed in deep water with water depth around 5 km.

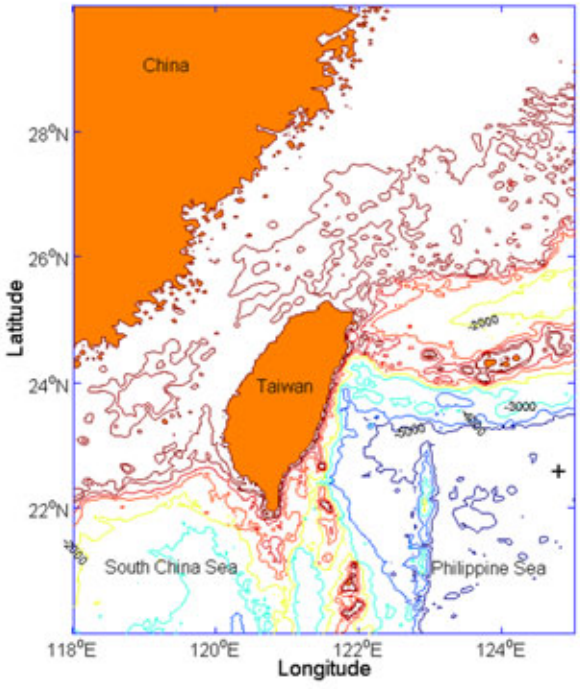

sound propagation can be effectively identified. Recently, ISWs were observed during 07:52–09:36 GMT July 30, 2005, in the Philippine Sea (water depth deeper than 5 km) near Taiwan (Figure 1) from the free drifting coastal monitoring buoy (CMB) (Figure 2) deployed by the U.S. Naval Oceanographic Office (Chu and Hsieh 2007a,b).

The original design of CMB was to collect data every 10 min near the air–ocean interface. Above the ocean surface, surface winds, air temperature, and air pressure were measured. Below the ocean surface, the temperature was observed at 1, 3, 5, 10, 15, and 20 m as shown in Figure 2. During the observational period (July 28–August 7, 2005), the CMB traveled 229.14 km along the track (Figure 3) with an average speed of 0.267 m/s. The surface winds were light, fluctuating from 3.3 m/s (minimum) to 4.2 m/s (maximum) with a mean wind speed of 3.8 m/s (Figure 4).

Sound Speed Profiles

During 07:52–09:36 GMT July 30, 2005, 10 temperature profiles were observed between 0 and 20 m from the CMB sensors (at 1, 3, 5, 10, 15, 20 m) with a sampling rate of 1/(10 min). About 424 temperature profiles were obtained between 25 and 140 m with sampling rate of 1/(15 s) from the fifteen thermistors attached to a wire rope from CMB (at 25, 30, 35, 40, 45, 50, 55, 60, 65, 70, 75, 80, 100, 130, 140 m). One temperature

FIGURE 2

The free drifting CMB used in the WPS survey. Fifteen thermistors are attached to a wire rope extending from the code of CMB (20 m deep) to 140 m with high-frequency sampling rate (every 15 s).

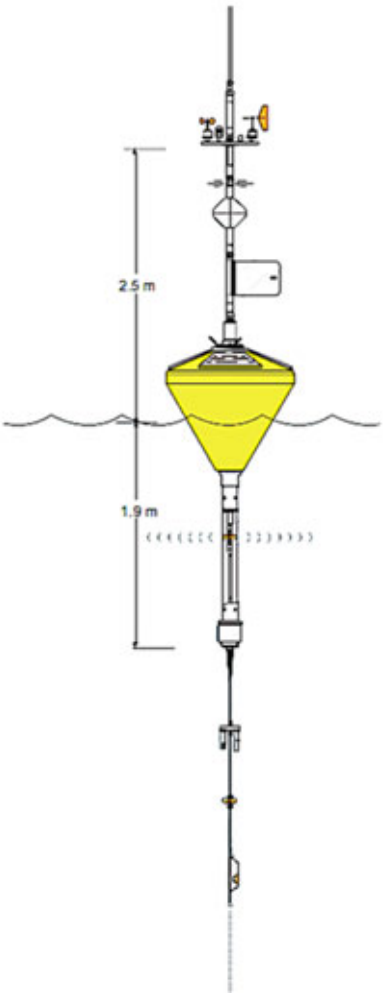

FIGURE 3

Track of CMB (from July 28 to August 7, 2005) deployed by the Naval Oceanographic Office.

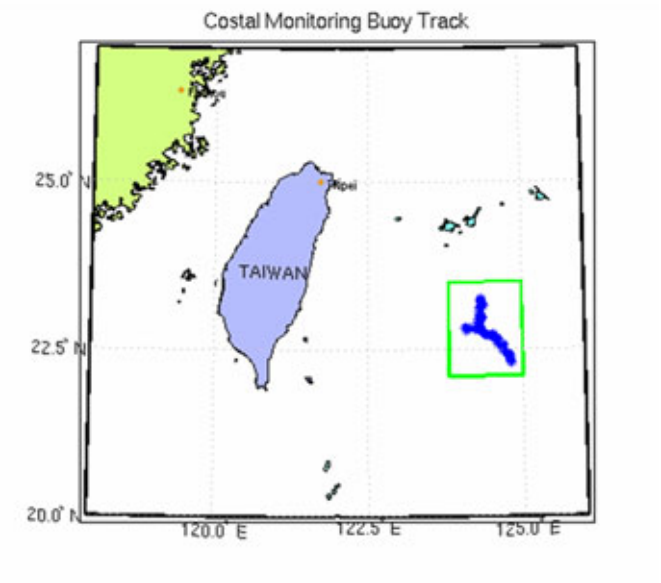

FIGURE 4

Wind speed during 0700–1200 GMT July 30, 2005, observed from CMB.

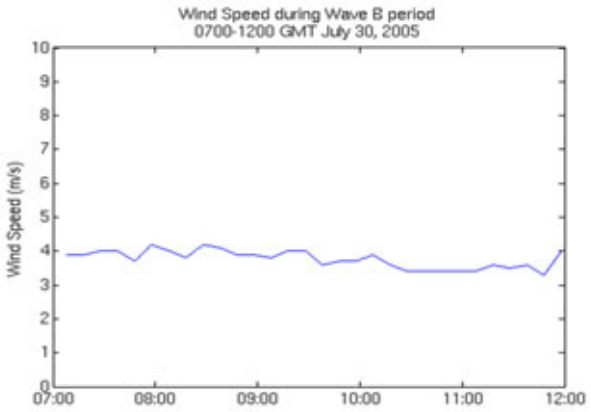

FIGURE 5

Mean SSP for range-independent simulation.

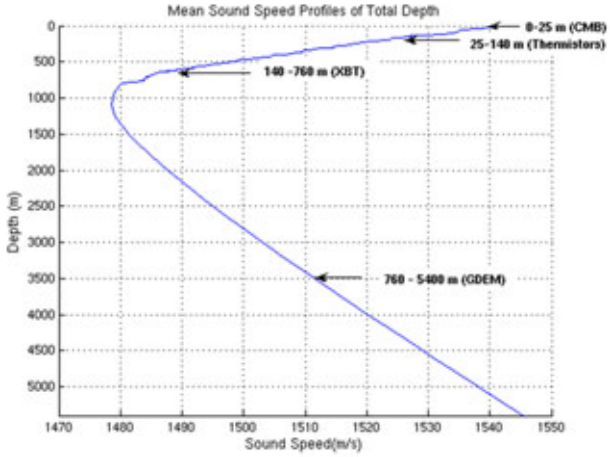

FIGURE 6

Sound speed between 25 and 140 m used for model simulation from the temperature field observed from 0752 to 0936 GMT July 30, 2005: (a) time-varying 424 SSPs and (b) depth–time cross section of the sound speed. Note that during the range-dependent acoustic simulation using CASS, the range-dependent portion of the SSPs was at depths between 25 and 140 m from 0752 to 0936 GMT July 30, 2005. Otherwise the SSP is the same as the mean profile shown in Figure 5.

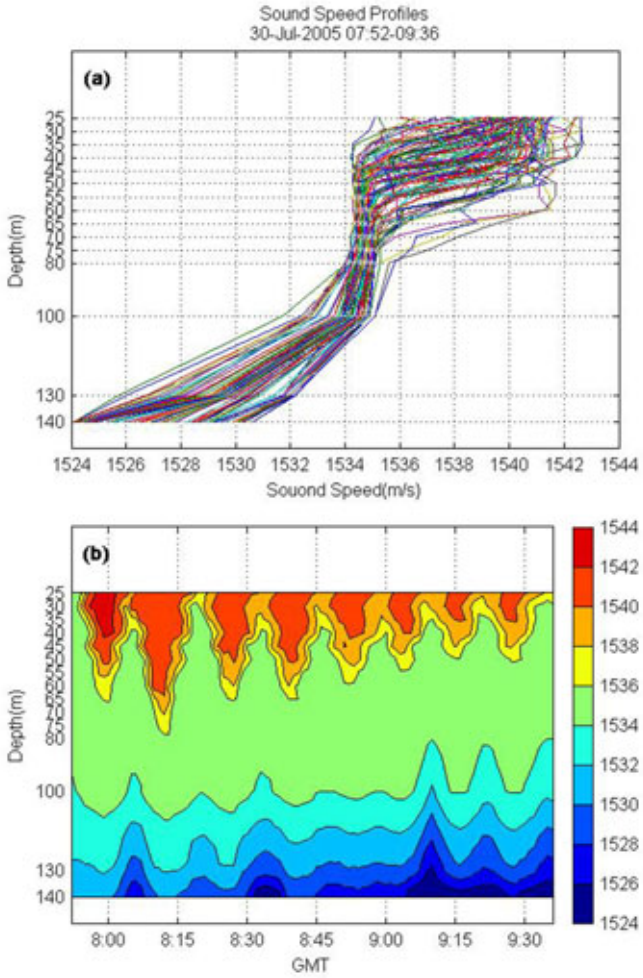

profile was used between 140 and 760 m from an expendable bathythermograph and one temperature profile below 760 m from the Navy's Generalized Digital Environment Model (GDEM) (average of July and August) nearest to the CMB.

The low-rate sampling data above 25 m (10 profiles) could not resolve propagation of ISWs. Below 140 m, only one profile was available. Thus, a temporally averaged profile was calculated from 10 profiles to represent the upper layer (above 25 m depth) thermal structure. The temporally invariant data in the upper layer (above 25 m) and the lower layer (below 140 m) was used for the whole observational period (07:52–09:36 GMT July 30, 2005). Thus, 424 temperature profiles from the surface to the bottom were obtained with temporal variation only between 25 and 140 m. Chu and Hsieh (2007b) identified the propagation of ISWs with a period of 7 min.

Salinity was not measured in this survey. To calculate sound speed, the GDEM (average of July and August) salinity profile (nearest to CMB) was used. The sound speeds calculated from the GDEM salinity profile and time average of 424 temperature profiles formed the mean sound speed profile (SSP) (Figure 5). The sound speeds calculated from the GDEM salinity profile and 424 temperature profiles generated the range-dependent SSPs (Figure 6). Comparison of the acoustic propagation between range-dependent and range-independent determined the effect of ISWs on acoustic propagation.

Modeling

Sonar Model

A range-independent generic sonar model has evolved into the Navy's

range-dependent Comprehensive Acoustic Simulation System with the Gaussian Ray Bundle eigenray model (CASS/GRAB) for acoustic and sonar analysis. It predicts range-dependent acoustic propagation in the frequency band between 600 Hz and 100 kHz (Weinberg and Keenan 1996; Keenan and Weinberg 2001). Test rays are sorted into families of comparable numbers of turning points and boundary interactions. Ray properties are power averaged for each ray family to produce a representative eigenray for that family. Target echo level and reverberation level are computed separately.

CASS/GRAB predicts the sonar performance reasonably well, given environmental input data such as bottom type, SSP, wind speed, and tilt angle of the sound source (Wagstaff and Keenan 2003). It has successfully modeled torpedo acoustic performance in shallow water exercises off the coast of Southern California and Cape Cod and is currently being developed to simulate mine warfare systems performance in the fleet (Keenan and Weinberg 1995; Chu and Vares 2004).

Model Integration

The Wilson (1960) equation for temperature–salinity–sound speed conversion is used. GRAB defaults to the Leroy equation (Leroy, 1969) for sound speed conversions, where numerically stable polynomials are fitted to Wilson's data. The environmental parameters for the CASS/GRAB input file (Naval Oceanographic Office System Integration Division, 1999a,b) consist primarily of data taken at the CMB buoy. The surface wind collected by the CMB during the ISW event is used as an input into CASS/GRAB. The water depth is 5,400 m. The bottom sediment type is silty clay without apparent layer structure from the Naval Oceanographic Office's database (Naval Oceanographic Office System Integration Division, 1999a). Bottom reflection effects are modeled using the Rayleigh scattering model. Two frequencies (3.75 and 7.5 kHz) with a bandwidth of 500 Hz and three source/transmitter depths (SD) (5, 100, and 200 m) are used. Eigenrays are generated in the mono-static active mode maximum surface/bottom reflections less than 30°. The vertical angle changes from –89° to 89° with the increment of 0.1°.

The calculated ISW propagation velocities are around 1.5 m/s. From 07:52 to 09:36 GMT July 30, 2005 (104 min), the ISWs traveled 9.36 km. It is noted that the estimate of spatial scale (i.e., 9.36 km) is based on the assumption of small propagation angles between the ISW propagation and the nominal acoustic direction. When the propagation angles are larger, these velocities can be much smaller, producing different length scales in which time variability may be predominant. Here, a range of 10 km is selected to investigate the ISW effects on the sound propagation.

ISW Effects

The CASS/GRAB model is primed with range-independent SSP (Figure 5) and range-dependent SSPs (Figure 6). Three source depths (5, 100, and 200 m) were chosen to place the source above, within, and below the thermocline. In addition, wind speed of 3.8 m/s, 0° source angle, and 10° Gaussian ray bundle were used as inputs for all of the CASS/GRAB model runs. We chose transmission loss (TL)

FIGURE 7

Transmission loss (left) and ray trace (right) from –10° and +10° of range-independent cases of f = 3.75 kHz at different source depths of (a) 5, (b) 100, and (c) 200 m.

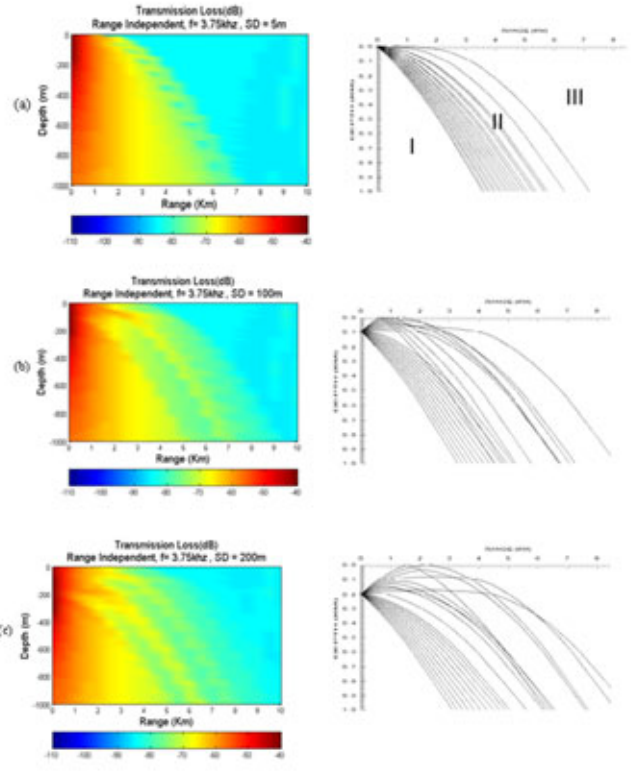

(an output from CASS/GRAB) as the primary parameter to investigate the ISW effects on sound propagation. Here, TL always takes on negative values.

Range-Independent

Range–depth cross section (range = 10 km; depth = 1000 m) is divided into three parts, with Area 2 being occupied by the Gaussian ray bundle (midrange). Left and right of Area 2 are defined by Area 1 (near range) and Area 3 (far range) (Figures 7a and 8a). For a range-independent SSP, the TL has distinct characteristics among the three areas: (1) weak TL for Area 1, (2) intermediate TL for Area 2, and (3) strong TL for Area 3. For f = 3.75 kHz, the TL varies from –40 to –65 dB for Area 1, from –65 to –73 dB for Area 2, and from –73 to –87 dB for Area 3 (Figure 7). For higher frequency (f = 7.5 kHz), the TL is comparable to that with lower frequency (f = 3.75 kHz) in Area 1 and Area 2 but enhances in Area 3 with varying from –78 to –90 dB (Figure 8).

TL Difference

The TL difference [Δ(TL)] between range-dependent ($TL_{dependent}$) and range-independent ($TL_{dependent}$) represents the ISW effect on sound propagation. Since TL is negative, the sound waves attenuate more because of ISWs when Δ(TL) < 0 and attenuate less when Δ(TL) > 0. The sound signal enhances little in Area 1 [i.e., Δ(TL) ~0–3 dB], weakens (up to –20 dB for SD = 5 m and –10 dB for SD = 100, 200 m) and enhances (up to 20 dB for SD = 5 m and 5–8 dB for SD = 100, 200 m) in Area 2, and weakens around –20 dB in Area 3 (Figure 9). Such a feature in Area 2 is very evident for the shallow sound source (SD = 5 m) and less evident for the deeper sound source (SD = 100, 200 m). However, a strong surface weakening zone with Δ(TL) ~–20 dB occurs for deeper sound source. The thickness of this surface weakening zone is around 15 m for SD = 100 m and 50 m for SD = 200 m. The evident weakening in Area 3 is for both frequencies and three SD values.

Since ISWs (usually for a two-layer fluid) can propagate at different angles (i.e., the crests of the ISWs might not be normal to the range–depth plane), the maximum value of |Δ(TL)| is a useful estimation of effect of ISWs on acoustic transmission. For a shallow source depth (SD = 5 m), the maximum value of |Δ(TL)| is 20 dB. For source depth at 100 and 200 m, the maximum TL reduction because of ISW propagation is –20 dB. These estimates could be used as a reference to assess the relevance of using the range-dependent estimate if Δ(TL) for each individual case falls outside this range, that is, the focusing errors might be larger than the time variability.

It is noted that the color contour plots (Figures 8 and 9) have significant steppy structures along rays. Such features occurred in a recent statistical study on the estimation of TL and its statistical properties on the basis of observations of ocean acoustic data acquired during the Asian Seas International Acoustics Experiment (ASIAEX) 2001 in the East China Sea (Dahl et al. 2004). During ASIAEX, the environmental parameters are first estimated. Then on the basis of the likelihood that each of these environmental models fits the ocean acoustic data, each model is mapped into TL. Such "steppy" may

FIGURE 8

Transmission loss (left) and ray trace (right) from –10° and +10° of range-independent cases of f = 7.5 kHz at different source depths of (a) 5, (b) 100, and (c) 200 m.

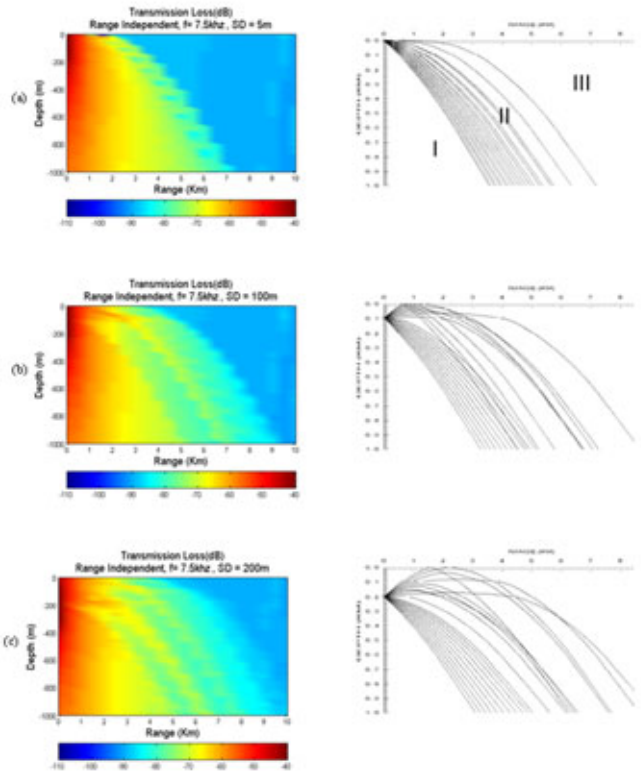

FIGURE 9

Effect of ISWs on acoustic transmission Δ(TL) (dB) with ISW propagation speed of 1.5 m/s for (a) source depth of 5 m and f = 3.75 kHz, (b) source depth of 5 m and f = 7.5 kHz, (c) source depth of 100 m and f = 3.75 kHz, (d) source depth of 100 m and f = 7.5 kHz, (e) source depth of 200 m and f = 3.75 kHz, and (f) source depth of 200 m and f = 7.5 kHz. Note that the sound waves attenuate more with ISWs than without ISWs For Δ(TL) < 0, and otherwise for Δ(TL) > 0.

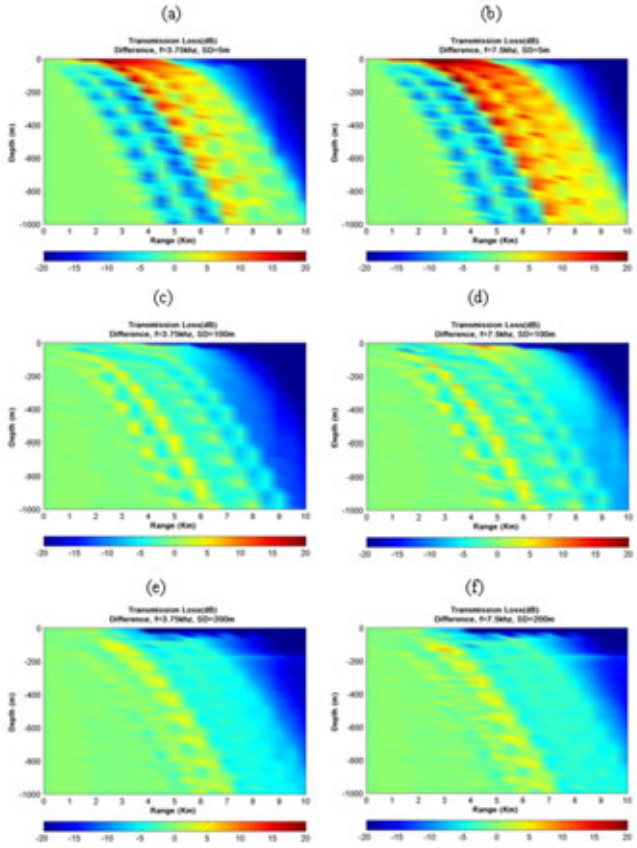

be caused by changing in amplitudes and separations of acoustic signals in such a way that the cumulative time integral of the pulse shape matches the more "steppy" cumulative integral of the true eigenray or mode arrival pulse shape.

Summary

(1) This study shows the impact of nonlinear internal waves in sonar performance estimation using the CASS/GRAB model with range-independent and range-dependent SSPs calculated from the high-frequency temperature observational data. ISWs strongly impact sound propagation with a basic pattern of little enhancement (0–3 dB) in near-range, alternate attenuation (up to –20 dB for SD = 5 m and –10 dB for SD = 100, 200 m) and amplification (up to 20 dB for SD = 5 m and 5–8 dB for SD = 100, 200 m) in midrange, and attenuation (up to –20 dB) in far range. An evident surface weakening zone exists in midrange with strongest Δ(TL) ~–20 dB for deep sound source (SD = 100, 200 m) but does not exist for shallow sound source (SD = 5 m). The thickness of this surface weakening zone is around 15 m for SD = 100 m and 50 m for SD = 200 m.

(2) We should be cautious to interpret these results because of the mean SSP profile calculated from 10 routine CMB measurements for the top layer (0–25 m). A large vertical gradient may be created at a depth of 25 m. Such a vertical gradient also occur in the range-independent case. The effect of such a vertical gradient may be offset because of the modeled differences in acoustic propagation between the range-independent and the range-dependent SSPs. In a future study, an ocean numerical model is needed to assimilate this observational data to get continuous temperature profiles from the surface to the bottom of the ocean.

(3) Although the modeling results reconcile previous measurements of transmission loss fluctuations near ISWs, it is pointed out that the complicated ISW effects on sound propagation in the Philippine Sea identified here using the CASS/GRAB model must be verified by acoustic observations. Experiments similar to the Asian Seas International Acoustics Experiment (ASIAEX) are needed for this region.

Acknowledgments

The Naval Oceanographic Office and the Naval Postgraduate School supported this study. The authors deeply thank Ms. Ruth E. Keenan from the Scientific Application International Corporation, Mashpee, Massachusetts, and Mr. Melvin D. Wagstaff at the Naval Oceanographic Office for their guidance on the CASS/GRAB modeling and simulation.

Lead Author:

Peter C. Chu
Naval Ocean Analysis and Prediction Laboratory

Naval Postgraduate School, Monterey, CA, 93493
Tel: 831-656-3688
Fax: 831-656-3686
E-mail: pcchu@nps.edu

References

Apel, J.R., Holbrook, J.R., Liu, A.K., Tsia, J.J. 1985. The Sulu Sea internal soliton experiment, J. Phys. Oceanogr. 15:1625-51. doi:10.1175/1520-0485(1985)015<1625:TSSISE>2.0.CO;2.

Chu, P.C., Hsieh, C.P. 2007a. Multifractal thermal characteristics of western Philippine Sea upper layer. Indian J. Mar. Sci. 36(2):141-51.

Chu, P.C., Hsieh, C.P. 2007b. Change of multifractal thermal characteristics in the western Philippine Sea upper layer during internal wave-soliton propagation. J. Oceanogr. 63(6):927-39. doi:10.1007/s10872-007-0078-6.

Chu, P.C., Vares, N.A. 2004. Uncertainty in shallow sea acoustic detection due to environmental variability. U.S. Navy J. Underw. Acoust. 54:347-67.

Dahl, P.H., Zhang, R., Miller, J.H., Bartek, L.R., Peng, Z.H., Ramp, S.R., Zhou, J.X., Chiu, C.-S., Lynch, J.F., Simmer, J.A., Spindel, R.C. 2004. Overview of results from the Asian Seas International Acoustics Experiment in the East China Sea. IEEE J. Oceanic Eng. 29:920-28. doi:10.1109/JOE.2005.843159.

Keenan, R.E., Weinberg, H. 2001. Gaussian ray bundle (GRAB) model shallow water acoustic workshop implementation. J. Comput. Acoust. 9:133-48. doi:10.1016/S0218-396X(01)00071-1.

Keenan, R., Weinberg, H. 1995. Torpedo reverberation data modeling with the Comprehensive Acoustic Simulation System (CASS). NUMC-NPT Technical Report 10. pp. 408. Newport, RI: Naval Undersea Warfare Center Division.

Leroy, C.C. 1969. Development of simple equations for accurate and more realistic calculation of the sound speed in sea water. J. Acoust. Soc. Am. 46(1):216-26. doi:10.1121/1.1911673.

Naval Oceanographic Office Systems Integration Division. 1999a. Software design document for the Gaussian Ray Bundle (GRAB) eigenray propagation model. Mississippi: OAML-SDD-74, Stennis Space Center. pp. 445.

Naval Oceanographic Office Systems Integration Division. 1999b. Software requirements specification for the Gaussian Ray Bundle (GRAB) eigenray propagation model. Mississippi: OAML-SRS-74. Stennis Space Center. pp. 40.

Rodriguez, O.C., Jesus, S., Stephan, Y., Demoulin, X., Porter, M., Coelho, E. 2000. Nonlinear soliton interaction with acoustic signals: focusing effects. J. Comput. Acoust. 8:347-63. doi:10.1016/S0218-396X(00)00025-X.

Wagstaff, M.D. and Keenan, R.E. 2003. Modeling the effects of surface sediments and small scale bathymetry upon high-frequency shallow water reverberation. In: Proceedings of MTS/IEEE OCEANS 2003. pp. 1070-71. San Diego, CA.

Weinberg, H., Keenan, R.E. 1996. Gaussian ray bundles for modeling high-frequency propagation loss under shallow water condition. J. Acoust. Soc. Am. 100(3):1421-31. doi:10.1121/1.415989.

Wilson, W.D. 1960. Equation for the speed of sound in sea water. J. Acoust. Soc. Am. 32:1357-67.doi:10.1121/1.1907913.

Zhou, J.X., Zhang, X.Z. 1991. Resonant interaction of sound wave with internal solitons in the coastal zone. J. Acoust. Soc. Am. 90:2042-54. doi:10.1121/1.401632.